DEUTSCHES ELEKTRONEN-SYNCHROTRON DESY

DESY SR-77/17
October 1977

Atomic and Molecular Effects in the VUV Spectra of Solids

by

B. Sonntag
II. Institut für Experimentalphysik, Universität Hamburg

NOTKESTRASSE 85 · 2 HAMBURG 52

To be sure that your preprints are promptly included in the
HIGH ENERGY PHYSICS INDEX ,
send them to the following address (if possible by air mail) :

DESY
Bibliothek
Notkestraße 85
2 Hamburg 52
Germany

Atomic and Molecular Effects in the VUV Spectra of Solids.

B. Sonntag

II. Institut für Experimentalphysik, Universität Hamburg

Hamburg Germany

abstract

The VUV spectra of solids are often dominated by atomic or molecular effects, which clearly manifest themselves in the gross features of the spectra and the fine structure at inner shell exitation thresholds. Evidence for the influence of atomic and molecular matrix elements, multiplet-splitting and correlation is presented. Special emphasis is given to the direct experimental verification based on the comparison of atomic and solid state spectra.

A introduction

The VUV spectra of solids are strongly influenced by localized excitations. Therefore the one-electron band model frequently fails to describe the spectra.[1-3] The approaches to overcome this difficulty can be grouped in two classes according to their starting points. The first class is based on the one-electron bandstructure. Local interactions are treated with the help of localized orbitals constructed from Bloch-states. The second class starts out with the states of the free atoms or molecules thereby incorporating intraatomic or intramolecular interactions already at the outset. The influence of the surrounding solid is taken into account by perturbation theory. Due to the small extension of core states core excitations only probe the wave functions close to the nucleus. Thus for core spectra atomic or molecular effects are expected to prevail and the latter approach promises a more direct insight in the nature of the excitations.

The main perturbations originate from the nearest shells of neighbouring atoms. Therefore cluster calculations capable of handling varying numbers of atoms seem to be ideally suited. Transfered to experimental physics this approach corresponds to synthesizing the spectra of the solids from the experimental spectra ot the atomic or molecular building blocks. The ideal experiment would start out with the determination of the spectrum of a single atom and then go on by successively adding atoms thus forming larger and larger clusters until the spectrum is identical with the spectrum of the solid. In reality this is not feasible in most cases, though the possibilities of matrix isolation spectroscopy or cluster formation in jet streams have not been fully exploited. Inspite of these limitations detailed information on the nature of the core excitations has been abtained by comparing the spectra of the solids with the corresponding spectra of the free atoms or molecules.

B gross features of inner shell absorption spectra

Core states (binding energy $>$ 2o eV) are confined within a narrow region around the nucleus. In the solid the atomic character of these states is preserved because core states of neighbouring atoms don't overlap . Optical transitions from core states only probe the final state within the region of overlap . For final states $>$ 2o eV above threshold the solid state wavefunctions can be approximated by the wave functions of the free atom within a small volume around the nucleus of the excited atom and plane waves outside. This means that only the interaction with the nucleus and the electrons of the excited atom has to be taken into account whereas the interactions with the other atoms in the crystal can be neglected. The validity of this approximation becomes clear if we remember that the outgoing electron wave has to be

orthogonalized to all occupied states of the surrounding atoms. This can be achieved by representing the atoms by their pseudopotentials. For final states more than 2o eV above threshold the kinetic energy of the electron is large compared to the variations of the pseudopotential which therefore can be replaced by a constant.
This explains why the gross features of the inner-shell absorption spectra of solids for photon energies > 2o eV above threshold are well reproduced by an atomic model. It is obvious that this model generally does not hold at threshold, where solid state effects are important, and fails to reproduce the oscillatory behaviour (EXAFS) of the absorption coefficient of molecules and solids extending far above threshold.

VUV absorption spectra of solids show all the features characteristic for the VUV spectra of atoms.

wide extension of the spectrum The inner-shell absorption spectra extend far above threshold.

dominance of the l→l + 1 transitions The oscillator strength of the l→l + 1 transitions is generally one ore two orders of magnitude larger than the oscillator strength of the l→l - 1. transitions.

delayed onset Often the absorption is suppressed at threshold by a centrifugal barrier. The spectrum reaches its maximum far beyond threshold.

resonance near threshold If nl→nl + 1, l l transitions are allowed within the same shell giant resonances show up ~ 2o eV above threshold. With increasing Z the resonance shifts towards threshold.

cooper minima If the initial wave funtion has nodes i. e. n > l + 1, the transition probability for nl → ε l + 1 transitions goes through zero above threshold.

The features listed above are well reproduced by one-electron models.[4] In these models the oscillator strength f(nl→εl'), averaged over all orientations, for transitions from an initial state with quantum numbers n, l to a final state with kinetic energy ε is given by

$$f(nl \rightarrow \varepsilon l') = \frac{2m(\varepsilon - E_{nl})}{3\hbar^2} \cdot \frac{l + l' + 1}{2(l+1)} R^2(nl, \varepsilon l')$$

where the matrix element

$$R(nl, \varepsilon l') = \int_0^\infty P_{nl}(r)\, r\, P_{\varepsilon l'}(r)\, dr$$

The wave function $P_{ne}(r)$ obeys the radial equation

$$\frac{d^2 P_{nl}(r)}{dr^2} + \frac{2m}{\hbar^2}\left(E_{nl} - V(r) - \frac{l(l+1)\hbar^2}{2mr^2}\right) P_{nl}(r) = 0$$

V(r) represents a realistic atomic potential obtained by selfconsistent-field calculations.

Fig. 1 shows the absorption spectra of atomic and solid Ar from threshold up to 5oo eV.[3] The excellent agreement between both spectra demonstrates the validity of the atomic model. Both spectra show the 3p → εd resonance at 25 eV, the Cooper minimum at 5o eV and the subsidiary 3p→εd maximum at 8o eV. There is similar agreement between the spectra of solid and gaseous Ne, Kr and Xe.[3]

The absolute photoabsorption cross sections in the single electron approximation differ considerably, sometimes by an order of magnitude, from the values given by experiment. These calculations give resonance maxima much narrower and at lower energies than found experimentally. These discrepancies have been proven to be due to many-electron correlations.

The absorption spectra of the atomic rare gases can be successfully described terms of the random phase approximation with exchange (RPAE).[5] The fact that atomic and solid state spectra almost coincide proves that the atomic correlation effects are essentially unaltered in the solid. In order to demonstrate that the validity of the atomic approach is not limited to solids bound by weak Van der Waals forces, the Cs-4d spectra of atomic Cs, Cs metal, crystalline and molecular CsCl are presented in Fig. 2.[6] There is a marked similarity between the four spectra. They are all dominated by the giant Cs 4d→εf resonance peaking ~30 eV above threshold.Except at threshold the theoretical cross section for atomic Cs abtained by RPAE[5] agrees with the experimental result. Due to the neglect of relaxation effects the theory predicts a higher 4d-threshold energy and a steeper rise of the cross section above the 4d-threshold than determined experimentally. The simultaneous exitation of one 4d and one 5p electron is responsible for the structures between 92 eV and 102 eV.

Photoelectron energy distributions (PED) from valence bands at a series of energies in the ultraviolet (UPS) and x-ray (XPS) regime often show marked differences in the relative strength of characteristic features, which have been attributed to a strong energy dependence of the dipole matrix element. Since high energy photoemission experiments emphasize the region close to the nucleus the energy dependence of atomic matrix elements can be used as guideline. This approach has turned out to be very promising. Using the characteristic energy dependence of atomic cross sections for transitions from the outer s, p, d and f states the symmetry character of the valence band state of various compounds has been determined from the $\hbar\omega$ dependence of the PEDs.[7,8] The PEDs of $MoTe_2$ measured at 21 eV, 35 eV and 1486 eV are presented as an example in Fig. 3.[9] According to McGovern and Williams[9] the total emission $N(E,\hbar\omega)$ (E = binding energy) can be factorized into photon energy independent symmetry

projected density of states Np(E), $N_d(E)$ and $\hbar\omega$ dependent cross section factors $Cp(\hbar\omega)$, $C_d(\hbar\omega)$.

$$N(E,\hbar\omega) = Cp(\hbar\omega)Np(E) + C_d(\hbar\omega)N_d(E)$$

The upper part of the valence band is formed by the Mo 4d states; the lower part is derived from the Te 5p states. Above the resonance near threshold the Te 5p cross section goes through a Cooper minimum, which is well reflected in the low intensity of the p-band at $\hbar\omega$ = 30 eV.

C molecular effects

We already mentioned that the atomic approach fails to describe the oscillatory behaviour of the cross section frequently detected in the absorption spectra of solids above inner-shell excitation thresholds. These oscillations are clearly to be seen in the 2p spectra of Na, Al[10] and Si.[11] The 2p spectra of atomic[12] and solid Al[10] are presented in Fig. 4. Above threshold the spectrum of atomic Al shows a gradual rise peaking at ~105 eV and than a slow decline with increasing photon energy. This spectral behaviour is in agreement with that of the calculated spectrum[13] and can be attributed to the delayed onset of the 2p→εd transitions. 2s excitations give rise to the asymmetric lines above 105 eV. The spectrum of Al metal shows the same general behaviour but the broad maxima at 97 eV and 120 eV have no counterpart in the atomic spectrum. Part of the maximum at 120 eV may be due to 2s excitations which are responsible for the small hump at 118 eV. Similar results have been obtained for Na.[14] The structures are clearly due to the influence of the surrounding atoms. Ritsko et al.[15] have shown that these structures can be interpreted as extended x-ray absorption fine structure (EXAFS). In EXAFS the final state Ψ_f close to the nucleus of the excited atom is described by the superposition of the outgoing atomic wave Ψ_a with the waves backscattered from the neighboring

atoms Ψ_{sc}.

$$\Psi_f = \Psi_a + \Psi_{sc}$$

The absorption cross section due to transitions from the initial state Ψ_i is given by

$$\sigma \sim |\langle \Psi_i | r | \Psi_a \rangle + \langle \Psi_i | r | \Psi_{sc} \rangle|^2$$

The first term squared gives the smoothly varying atomic cross section while the mixed term yields a contribution oscillating as a function of final state energy. In essence this oscillation is due to constructive and destructive interference between the outgoing atomic and the back-scattered waves at the position of the excited atom. According to Ritsko et al.[15] it is sufficient to perform the calculations for a small cluster comprising the nearest neighbours of the excited atom. The simplicity of the model applied by these outhers precludes the exact determination of the size of the cluster necessary to reproduce the experimental spectrum. Multiple scattering calculations for clusters of varying size based on realistic pseudopotentials and taking the effect of the core hole into account see to be very promising for this purpose. These calculations are by no means trivial but they offer unique advantages for the treatment of inner-shell excitations. Based on the present knowledge it is safe to assume that the essential features of the spectra are determined by only a few shells of nearest neighbours, and thus can be considered "quasi molecular".

For molecular crystals like solid SiF_4 the molecular origin of the corresponding broad peaks above the Si-2p threshold can be verified experimentally.[15] The broad bands above threshold are present in the spectra of molecular and solid SiF_4 given in Fig. 5. These bands are ascribed to the modulation of the transition matrix element caused by the superposition

of the outgoing wave and the waves backscattered by the F ligands. The interpretation of the bands in term of resonances localized within the cage formed by the F ligands is equivalent to this.[17] Scattering by the nearest Si neighbours is probably responsible for the weak absorption band at 143 eV in the spectrum of solid SiF_4. The appearance of a similar band in the spectrum os solid SiH_4 supports this assignment.[16] The small scattering amplitude of H explains why the resonances are missing in the spectra of solid and molecular SiH_4.[16,18]

D structure at inner-shell thresholds

So far we have left out the region close to inner-shell thresholds, where solid state effects dominate in many cases. Van der Waals solids are predestinated for the search for atomic or molecular effects at threshold. Fig. 6 shows the absorption of molecular and solid SiH_4 close to the Si 2p-threshold.[16,18] Si $2p_{1/2,\ 3/2} \rightarrow 6^*(4a_1), 6^*(3f_2)$ core to valence state transitions give rise to the broad absorption band between 102,5 eV and 104,5 eV[19,20]. Transitions to s and d symmetric Rydberg states, converging to the series limits at 107,2 eV and 107,8 eV are reponsible for the sharp lines above 104 eV. These lines are completly smeared out in the solid whereas the prominent absorption band is only slightly broadened. A deconvolution of this absorption band shows that the intensity ratio of the $2p_{3/2} \rightarrow 6^*(4a_1)$, $2p_{1/2} \rightarrow 6^*(4a_1)$ transitions deviates considerably from the expected 2:1. This effect can be ascribed to the exchange interaction between the 2p-hole and the excited electron. In addition to the persistence of the maximum in the spectrum of solid SiH_4, this forms a strong evidicence for the localized nature of the excitations. There is also close correspondence between the fine structure at inner-shell thresholds for atomic and solid rare gases[3] and for molecular and crystalline alkali-halides.[6] Recently the ligand field model has been successfully applied to the interpretation of the structure at inner-shell absorption thres-

holds of alkali-halides[21] and to the x-ray emission[22] and photoemission[22,23] of transition metal compounds. The strong ionic multiplet splitting is incorporated by taking ionic spin-orbit, Coulomb and exchange interactions into account. The influence of the neighbouring ions is included via the field produced by them at the position of the excited ion.

The 4d-spectra of rare-earths metals form the most striking example for the importance of atomic effects at inner-shell thresholds.[24-26] The 4d-absorption of atomic and metallic Ce[27] in the energy range from 100 eV to 150 eV is shown in Fig. 7. There is an excellent agreement between the spectra of both phases. Details of the fine structure at the 4d-threshold of atomic and metallic Ce are given in Fig. 8. The agreement between the two spectra is almost perfect. The energies of most of the maxima showing up in the spectra of atomic and metallic Ce agree within the experimental errors. $4d^{10}4f\ 5s^2\ 5p^6\ 5d\ 6s^2 \rightarrow 4d^9\ 4f^2\ 5s^2\ 5p^6\ 5d\ 6s^2$ transitions determine the spectrum of atomic Ce. The strong Coulomb ($F_2(4d, 4f)$, $F_4(4d, 4f)$ and exchange ($G_1(4d, 4f)$, $G_3(4d, 4f)$, $G_5(4d, 4f)$ interactions give rise to a multiplet splitting of more than 20 eV. The highest levels, which comprise most of the oscillator strength are raised above the ionization limit.[28,29] This is borne out by the results of intermediate coupling calculations[27] of the multiplet splitting and relative oscillator strength for the Ce $4d^{10}4f\ 5s^2\ 5p^6\ 5d\ 6s^2(^1G_4) \rightarrow 4d^9\ 4f^2\ 5s^2\ 5p^6\ 5d\ 6s^2$ transitions to all J=3,4,5 final states included in Fig. 7 and Fig. 8. To facilitate comparison with the experimental data the 461 lines have been convoluted with a Lorentzian of 0,2 eV halfwidth. The interaction of the highest multiplet levels with the underlying continua gives rise to the giant resonance at 125 eV. The importance of many-electron correlations which are essentially unchanged in the solid is obvious. The rearrangement of the outer 5d and 6s electrons hardly influences the spectra. In addition to the experimental results this is supported by the calculation of the $4d^{10}4f \rightarrow 4d^9 4f^2$ transitions of the

Ce^{3+} ion.[29]

The interaction between a vacancy in the 4d-shell and the partly filled $4f^n$ shell also manifests itself in the soft x-ray emission spectra of rare-earths.[30] The emission spectra for La, Sm, Gd, Ho and Lu, corrected for bremsstrahlung contribution are shown in Fig. 9. Electron bombardement of rare-earths with the configuration $4d^{10}4f^n\ 5s^2\ 5p^6$ (outer electrons omitted) can

i) promote a 4d electron to the continuum $4d^{10}4f^n\ 5s^2\ 5p^6 \rightarrow 4d^9\ 4f^n\ 5s^2\ 5p^6$

ii) transfer a 4d electron to an empty 4f state.

$$4d^{10}4f^n\ 5s^2\ 5p^6 \rightarrow 4d^9\ 4f^{n+1}\ 5s^2\ 5p^6$$

Transitions from both states thus created contribute to the soft x-ray emission. For $1 \leq n \leq 14$ the multiplet components of these states are spread over $\sim$20 eV. The multiplet splitting of the $4d^9\ 4f^n\ 5s^2\ 5p^6$ states (case i) causes the complicated structure of the 4d x-ray photoemission spectra.[31] Since the $4d^9\ 4f^n\ 5s^2\ 5p^6$ and the $4d^9\ 4f^{n+1}\ 5s^2\ 5p^6$ multiplets overlap it is difficult to disentangle their contributions to the emission. Zimkima et al.[30] ascribed the emission band A to the transitions

$$4d^9\ 4f^n\ 5s^2\ 5p^6 \longrightarrow 4d^{10}\ 4f^n\ 5s^2\ 5p^5$$
$$4d^9\ 4f^{n+1}\ 5s^2\ 5p^6 \rightarrow 4d^{10}\ 4f^{n+1}\ 5s^2\ 5p^5$$

The multiplet splitting is responsible for the considerable width of the band. For Cs there is no multiplet splitting because of the drastically reduced overlap of the 4d and 4f wave functions. The corresponding emission band therefore can be resolved into three narrow components due to the $N_5 \rightarrow O_3$, $N_4 \longrightarrow O_2$, O_3 transitions. The wide emission band above B has been assigned to two types transitions

i) $4d^9\ 4f^n\ 5s^2\ 5p^6 \rightarrow 4d^{10}\ 4f^{n-1}\ 5s^2\ 5p^6$

ii) $4d^9\ 4f^{n+1}\ 5s^2\ 5p^6 \rightarrow 4d^{10}\ 4f^n\ 5s^2\ 5p^6$

Because of the high absorption above the 4d threshold part of the structures my be due to self-absorption though 1,5 keV electrons have been used for excitation. The sharp La emission lines at 97,3 and 101,7 eV exactly coincide with the lowest (La^{3+} $^1So \rightarrow {}^3P_1$, $^3D_1$) 4d absorption lines. This proves that reemission takes place. With increasing Z, i.e. filling of the 4d shell, the intensity ratio of the 4d $\rightarrow$ 4f emission to the 4d $\rightarrow$ 5p emission increases. For Lu band A is hardly detectable. In contrast to the spectra of La -- Tm the Lu 4d $\rightarrow$ 4f emission gives rise to two narrow, well resolved bands, which are separated by the spin-orbit splitting of the $4d_{5/2,\ 3/2}$ levels.[31] The 4f shell of Lu is completely filled and therefore there is no multiplet splitting due to the 4d — 4f interaction.

Multiplet splitting is also expected to influence the inner-shell spectra of transition metals, though the outer d-states are less localized than the 4f states of the rare earths. The complicated behavior of the electrical, optical and magnetic properties of transition metals is due to the partly local and partly itinerant character of the outer d-states. At threshold of the 3p-excitation the absorption spectra of the 3d-metals exhibit a strong asymmetric absorption band.[32-35] The width of this band by far exceeds the width of the empty part of the 3d-band. In analogy to the rare earths this band has been attributed to $3p^6\ 3d^n \rightarrow 3p^5\ 3d^{n+1}$ (outer electrons emitted) transitions split by the interaction of the partly filled d shell with the 3p-hole. Dietz et al.[34] and Davis and Feldkamp[35] have shown that the inclusion of a Fano type interference effect between the $3p^6\ 3d^n \rightarrow 3p^5\ 3d^{n+1}$ and the $3p^6\ 3d^n \rightarrow 3p^6\ 3d^{n-1}\ \varepsilon f$ transitions is essential, because $3p^5\ 3d^{n+1}$ autoionizes into $3p^6\ 3d^{n-1}\ \varepsilon f$ via super Coster-Kronig transition. Fig. 10 shows the 3d-absorption spectra of atomic and metallic Fe, Co and Ni.

The validity of the atomic approach is borne out by the close correspondence between the gross features of the spectra of both phases. Similar results have been obtained for Mn.[36] But in contrast to the 4d spectra of the rare earths there are marked differences between the spectra clearly manifesting the partly itinerant nature of the 3d electrons. The atomic spectra show sharp lines and broad structures which are absent in the spectra of the metals. Part of these structures are reproduced by the calculations performed by Davis and Feldkamp[35], but the relative energy positions and oscillator strengths deviate considerably from the experimental results.

References

1.) Kunz C. in : Optical Properties of Solids-New Developments, ed. B.O. Seraphin (North-Holland, Amsterdam, New York 1976) p. 473

2.) Koch E.E., Kunz C.and Sonntag B., Phys. Reports 29c (1977) 153

3.) Sonntag B. in : Rare Gas Solids, Vol. 2, eds, M.L. Klein and J.A. Venables (Academic Press, 1977)

4.) Fano U. and Cooper J.W., Rev.Mod.Phys. 4o (1968) 441 and 41 (1969) 724

5.) Amusia M.Ya. in : Vacuum Ultraviolet Radiation Physics, eds. E.E. Koch, R. Haensel and C. Kunz, (Vieweg/Pergamon, Braunschweig, 1974) p.2o5

6.) Radler K. and Sonntag B. Chem.Phys.Letters 39 (1976) 371

7.) Goldman A., Tejeda J. Shevchik N.J. and Cardona M., Phys.Rev. B1o (1974) 4388

8.) Eastman D.E. and Freeout J.L., Phys.Rev.Letters 7 (1975) 395

9.) McGovern I.T. and Williams R.H., Daresbury Laboratory DL/SRF/P32 submitted J.Phys.C. 1976 May

1o.) Haensel R., Keitel G., Sonntag B., Cunz C. and Schreiber P., phys.stat.sol. 2a (197o) 85

11.) Gähwiller and Brown F.C., Phys.Rev. B2 (197o) 1918

12.) Bruhn R. Diplomarbeit Universität Hamburg 1975

13.) McGuire E.J., SC-PR-7o-721, Sandia Laboratories, Albuquerque New Mexico 197o

14.) Wolff H.W., Radler K., Sonntag B. and Haensel R., Z.Phys. 257 (1972) 353

15.) Ritsko J.J., Schnatterly S.E. and Gibbons P.C., Phys.Rev.Letters 32 (1974) 671

16.) Friedrich H., Diplomarbeit Universität Hamburg 1976

17.) Dehmer J.L. and Dill D., Proceedings of the 2nd International Conference on Inner-Shell Ionization Phenomena, Freiburg 1976

18.) Hayes W. and Broun F.C., Phys.Rev. A6 (1972) 21

19.) Schwarz W.H.E., Chem.Phys. 11 (1975) 217

2o.) Schwarz W.H.E., Chem.Phys. 9 (1975) 157

21.) Satoko C. and Sugano S., J.Phys.Soc. Japan 34 (1973) 7o1

22.) Asada S., Satoko C. and Sugano S., J.Phys.Soc. Japan 37 (1975) 855

23.) Yamaguchi T. and Sugano S., J.Phys.Soc. Japan 42 (1977) 1949

24.) Fomichev V.A., Zimkina T.M., Cribovskii S.A. and Zhukova I.I., Soviet Phys. Solid State 9 (1967) 1163

25.) Zimkina T.M., Fomichev V.A., Cribovskii S.A. and Zhukova I.I., Soviet Phys. Solid State 9 (1967) 1128

26.) Mansfield M.W.D. and Connerade J.P., Proc.Roy.Soc. London A 352 (1976) 125

27.) Wolff H.W., Bruhn R., Radler K. and Sonntag B., Phys.Letters 59A (1976) 67

28.) Dehmer J.L., Starace A.F., Fano U., Sugar J. and Cooper J.W., Phys.Rev.Letters 26 (1971) 1521

29.) Sugar J., Phys.Rev. B5 (1972) 1785

3o.) Zimkina T.M., Fomichev V.A. and Cribovskii S.A., Sov.Phys. Solid State 15 (1974) 1786

31.) Padalia B.D., Lang W.C., Norris P.R., Watson L.M. and Fabian D.J., Proc.Roy.Soc. London A354 (1977) 269

32.) Sonntag B., Haensel R. and Kunz C.,
Solid State Commun. 7 (1969) 597

33.) Wehenkel C. and Gauthe B., Phys.Letters 47A (1974) 253

34.) Dietz R.E., McRae E.G., Yafet Y. and Caldwell C.W.,
Phys.Rev.Letters 33 (1974) 1372

35.) Davis L.C. and Feldkamp L.A.,
Solid State Communucations 19 (1976) 413

36.) Connerade J.P., Mansfield M.W.D. and Martin M.A.P.,
Proc.Roy.Soc. London A35o (1976) 4o5

Figure Captions

Fig. 1 Absorption coefficient of solid (solid line) and gaseous Ar (from ref. 3)

Fig. 2 Cs 4d absorption of molecular and crystalline CsCl, Cs metal and atomic Cs. The cross sections calculated by Amusia[5] for the 4d absorption ···· , for the contributions of the outer shells — ·· — ·· — and the total cross section are included. (from ref. 6)

Fig. 3 Photoelectron spectra for α-$MoTe_2$ for several photon energies. Binding energies are with respect to the valence band edge. The partial d – – – and p —·—·— emissions are included. (from ref. 9)

Fig. 4 2p-absorption of atomic and metallic Al. The spectrum calculated by McGuire[13] is included. (from ref. 12)

Fig. 5 Si-2p absorption of solid and molecular SiH_4 and SiF_4. (from ref. 16)

Fig. 6 Fine structure at the Si-2p threshold of solid[16] and molecular SiH_4 [18].

Fig. 7 4d-absorption of atomic and metallic Ce in the energy range from 1oo eV to 15o eV. The calculated spectra Ce $4d^{1o}$ 4f $5s^2$ $5p^6$ 5d $6s^2 \rightarrow$ $4d^9$ $4f^2$ $5s^2$ $5p^6$ 5d $6s^2$ (solid line) and Ce^{3+} $4d^{1o}$ 4f $5s^2$ $5p^6 \rightarrow 4d^9$ $4f^2$ $5s^2$ $5p^6$ (ref. 29, dashed line) are included. (from ref. 27)

Fig. 8 Fine structure at the 4d threshold of atomic and metallic Ce. The calculated spectra Ce $4d^{1o}$ 4f $5s^2$ $5p^6$ 5d $6s^2 \rightarrow$ $4d^9$ $4f^2$ $5s^2$ $5p^6$ 5d $6s^2$ (solid line) and Ce^{3+} $4d^{1o}$ 4f $5s^2$ $5p^6 \rightarrow 4d^9$ $4f^2$ $5s^2$ $5p^6$ (ref. 29, multiplied by o,5 , dashed line) are included. (from ref. 27)

Fig. 9 Soft x-ray emission spectra of La, Sm, Gd, Ho and Lu.[30]

Fig. 10 3p-absorption of atomic (solid line) and metallic[32] (dasked line) Fe, Co and Ni. The spectra calculated by Davis and Feldkamp[35] are given by the dotted line.

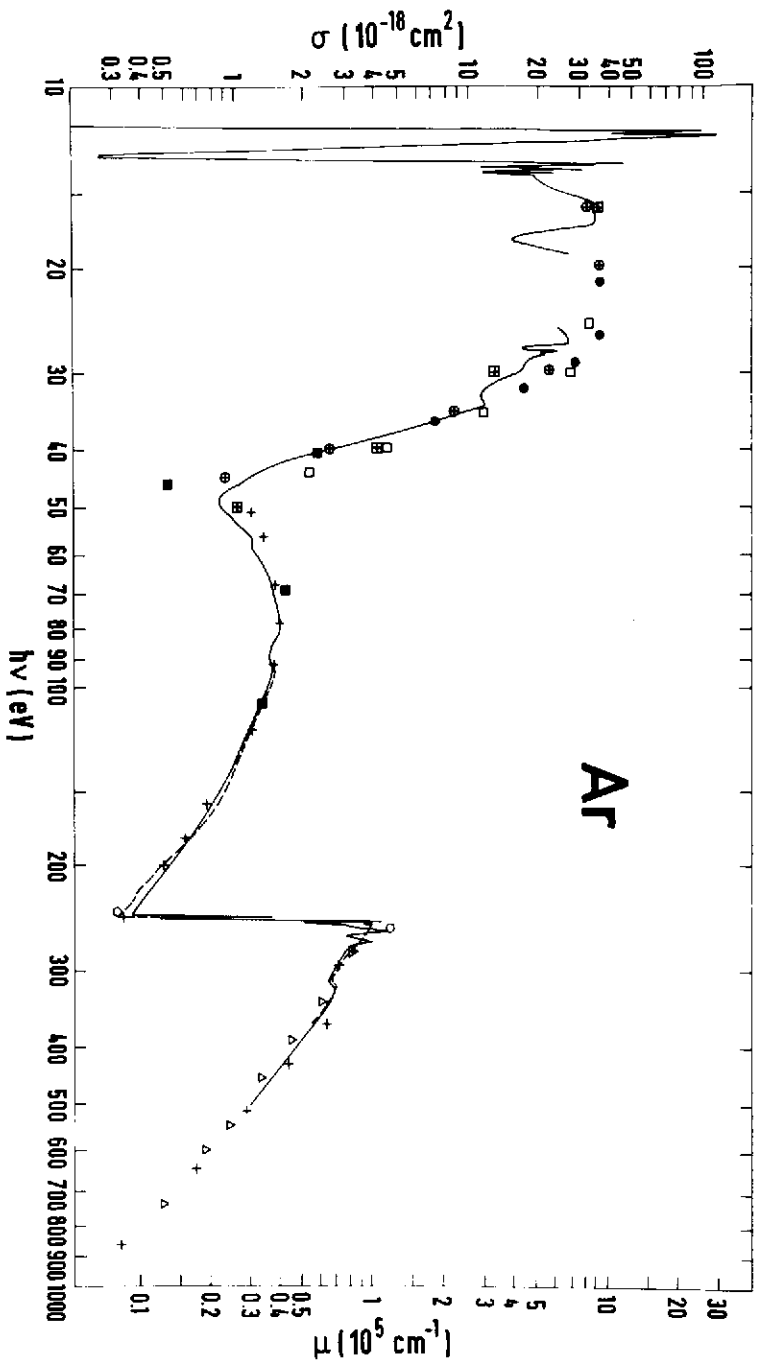

Fig. 1

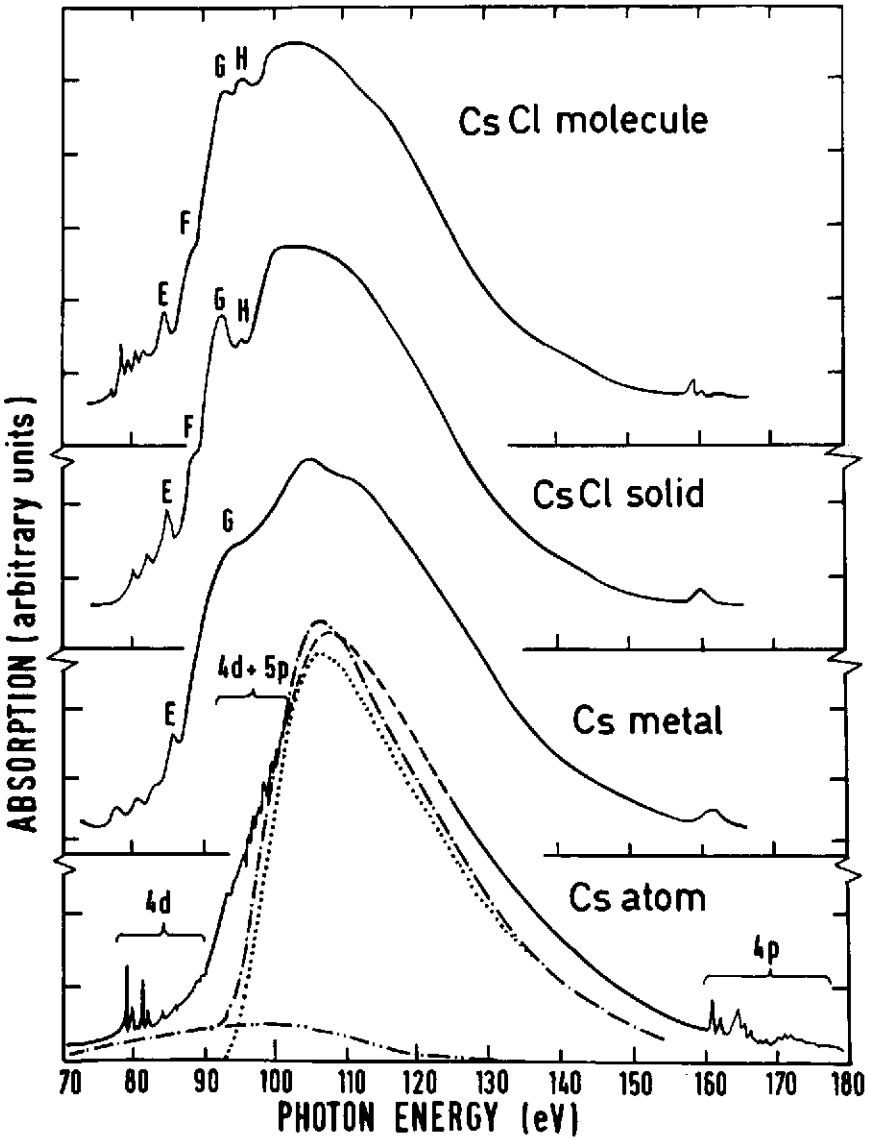

Fig. 2

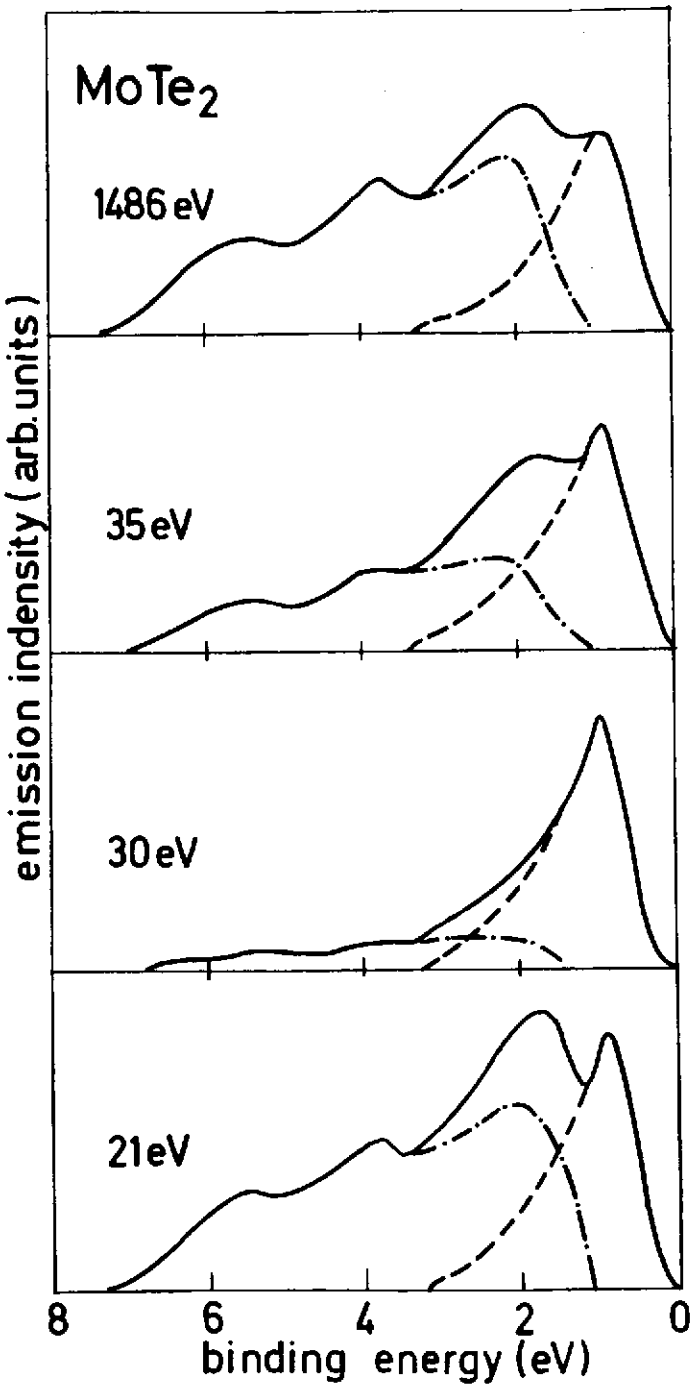

Fig. 3

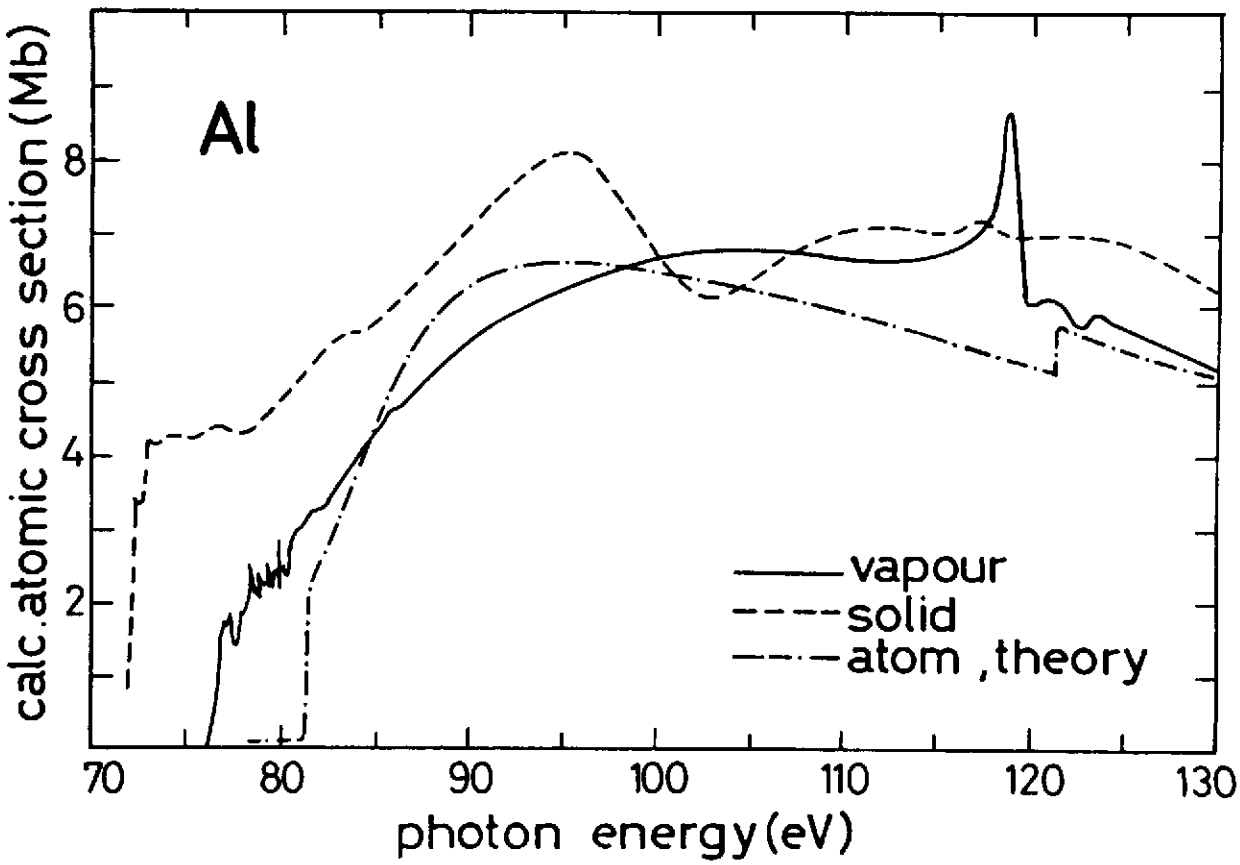
Al
calc.atomic cross section (Mb)
photon energy (eV)
vapour
solid
atom , theory

Fig. 4

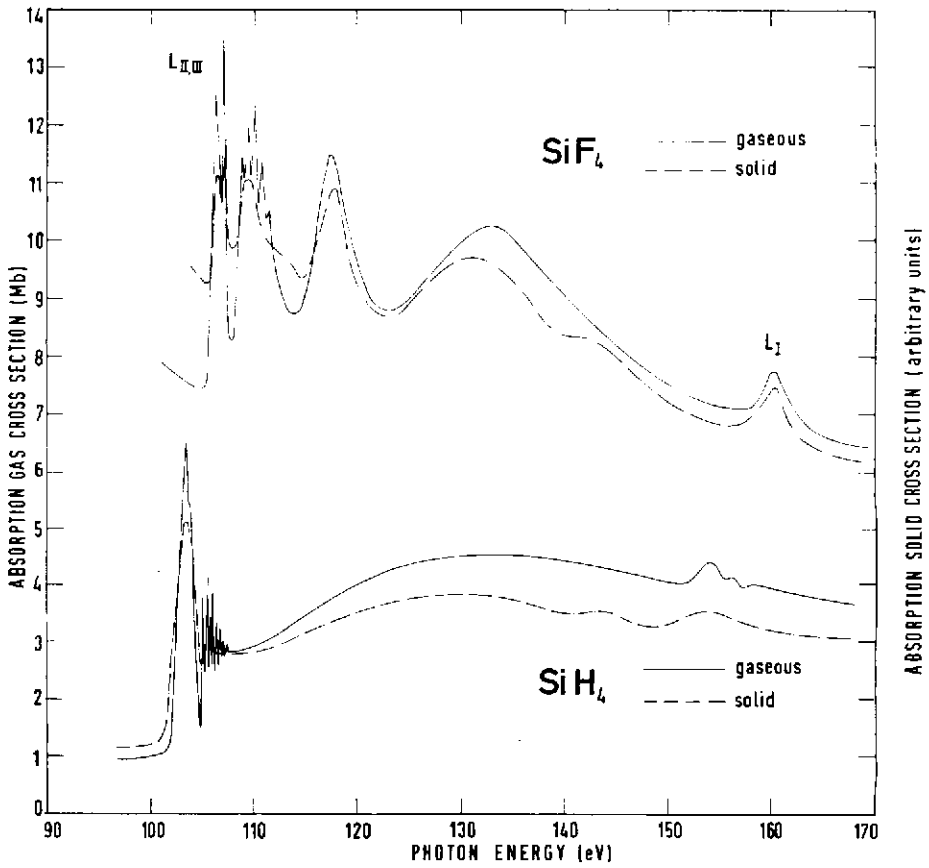
$L_{II,III}$
SiF_4
gaseous
solid
L_I
SiH_4
gaseous
solid
ABSORPTION GAS CROSS SECTION (Mb)
ABSORPTION SOLID CROSS SECTION (arbitrary units)
PHOTON ENERGY (eV)

Fig. 5

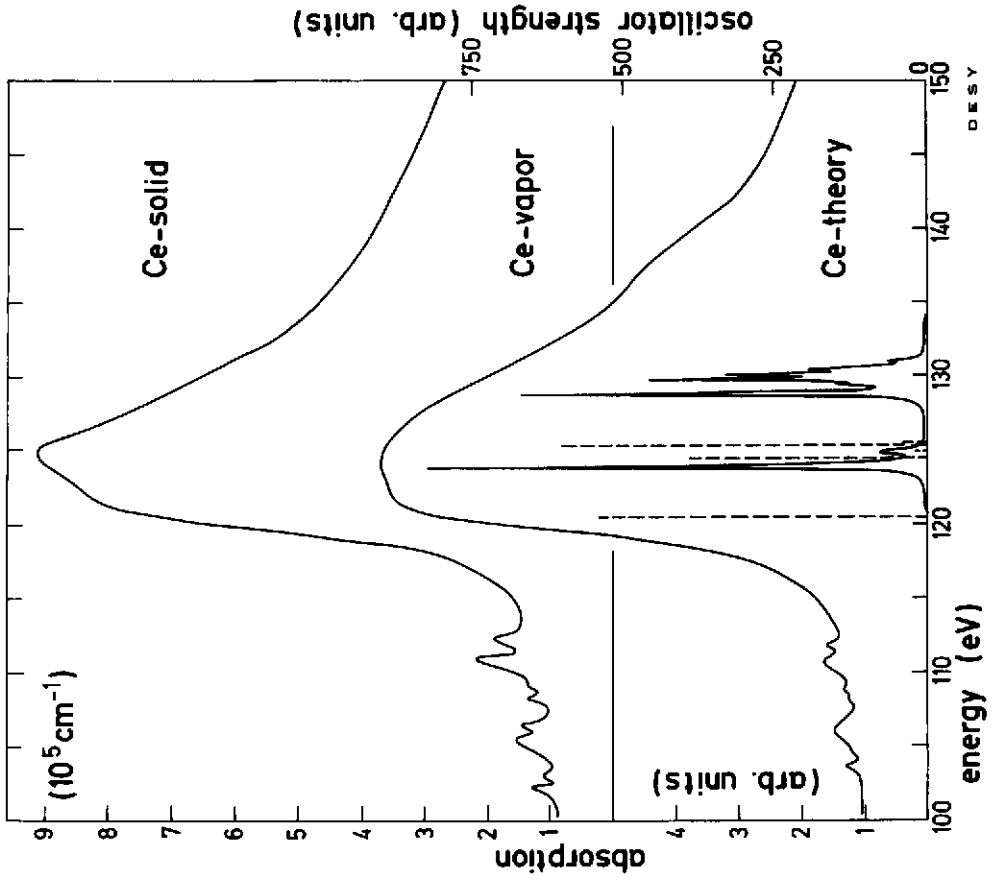
oscillator strength (arb. units)
750
500
250
0
DESY
25190
Ce-solid
Ce-vapor
Ce-theory
150
140
130
120
110
100
energy (eV)
(arb. units)
(10^5 cm^-1)
absorption
9
8
7
6
5
4
3
2
1
4
3
2
1

Fig. 7

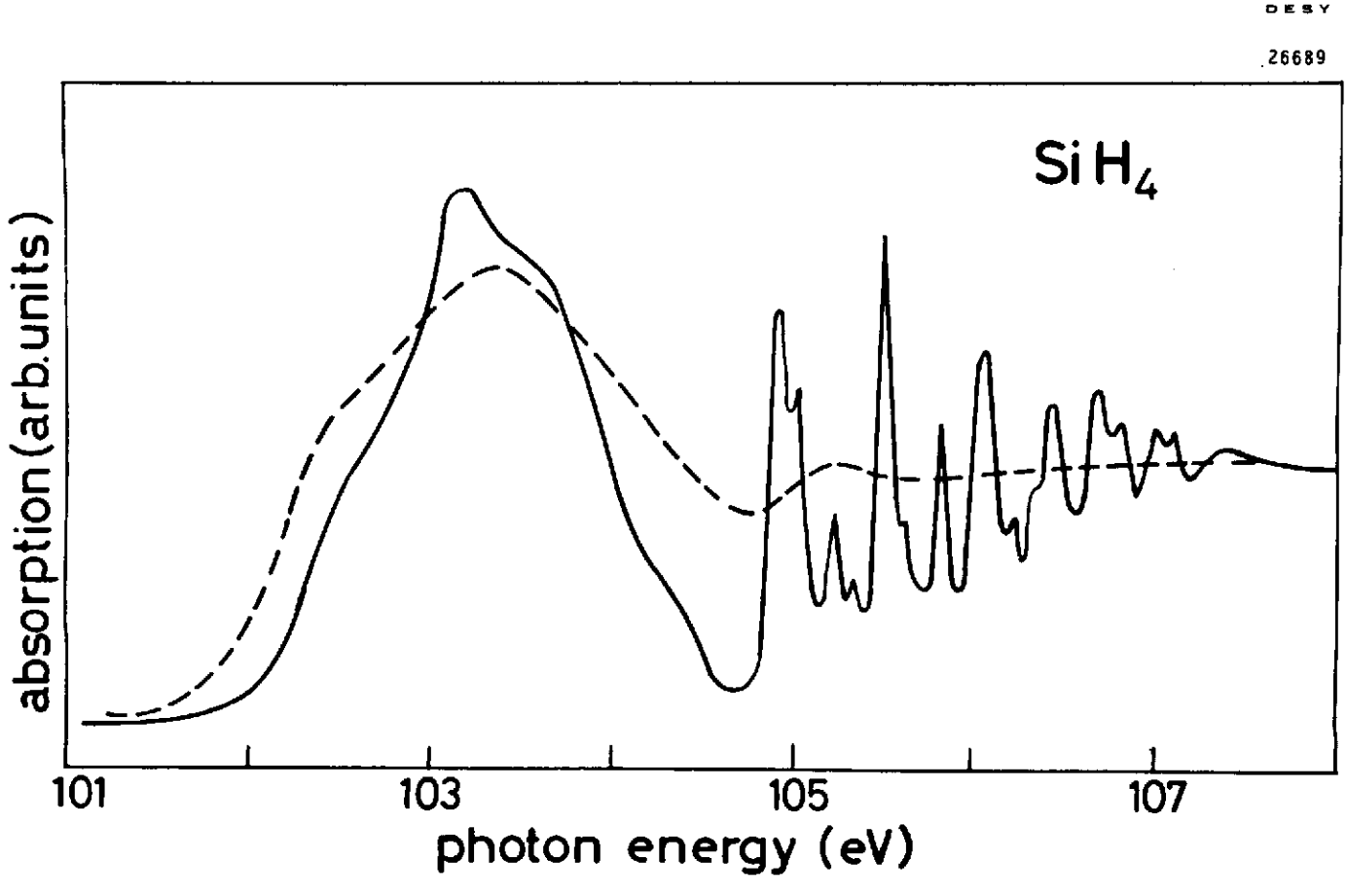
DESY
26689
Si H4
absorption (arb.units)
101
103
105
107
photon energy (eV)

Fig. 6

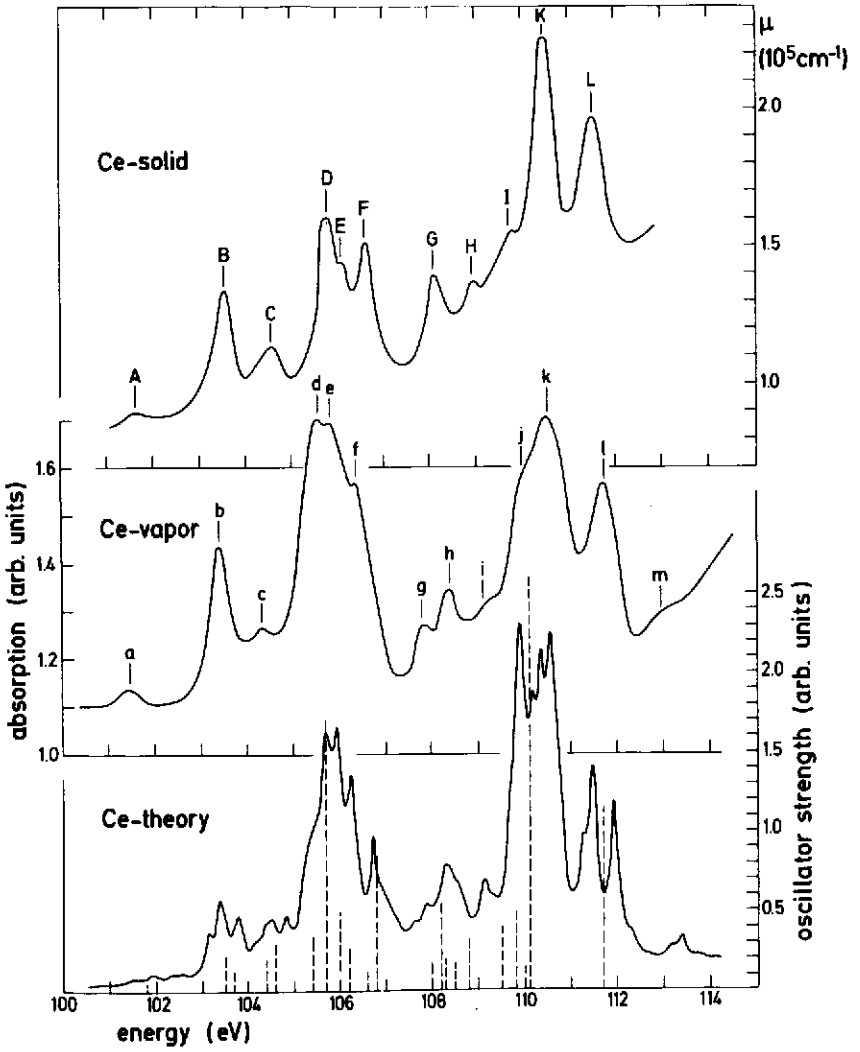
Ce-solid
Ce-vapor
Ce-theory
absorption (arb. units)
oscillator strength (arb. units)
μ (10⁵cm⁻¹)
energy (eV)

Fig. 8

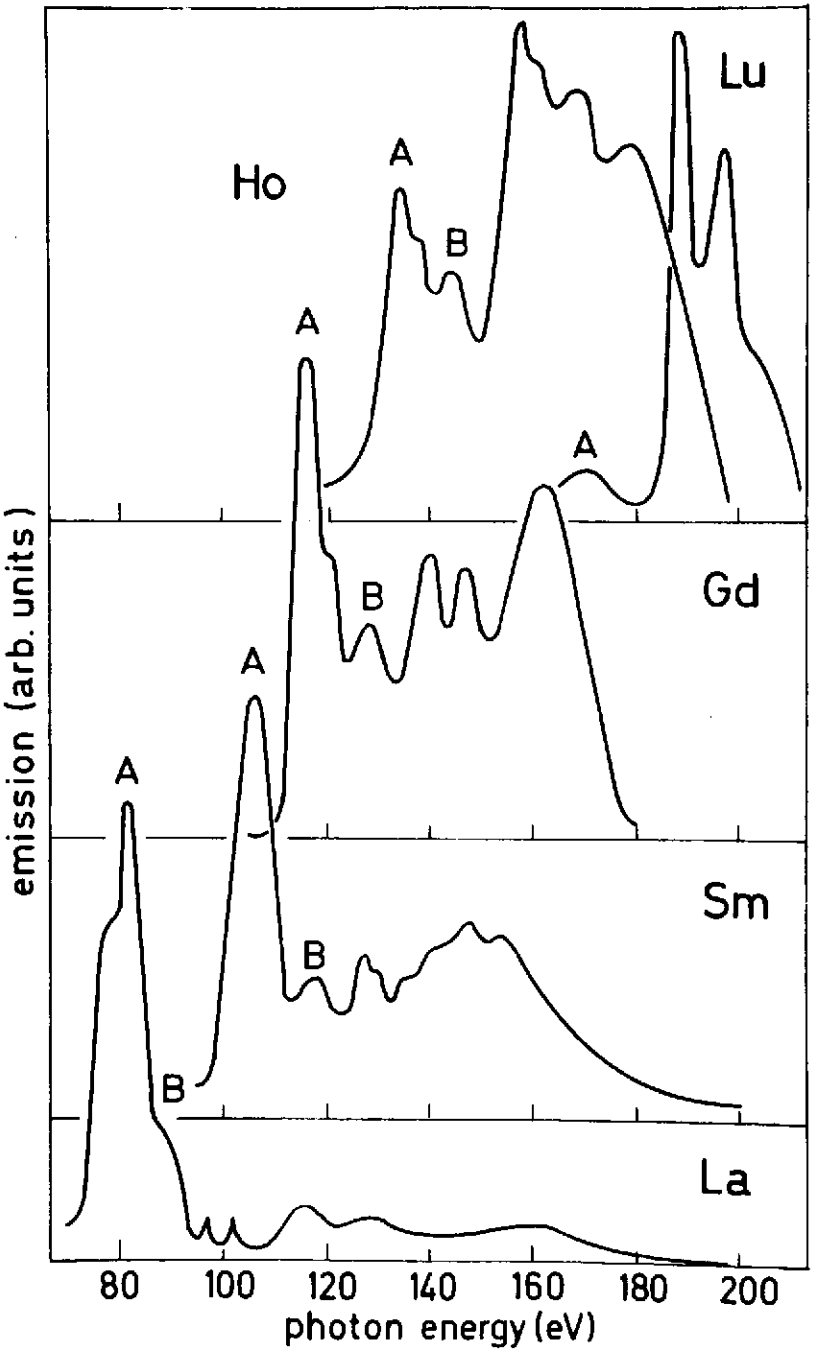
Lu
Ho
Gd
Sm
La
emission (arb. units)
photon energy (eV)

Fig. 9

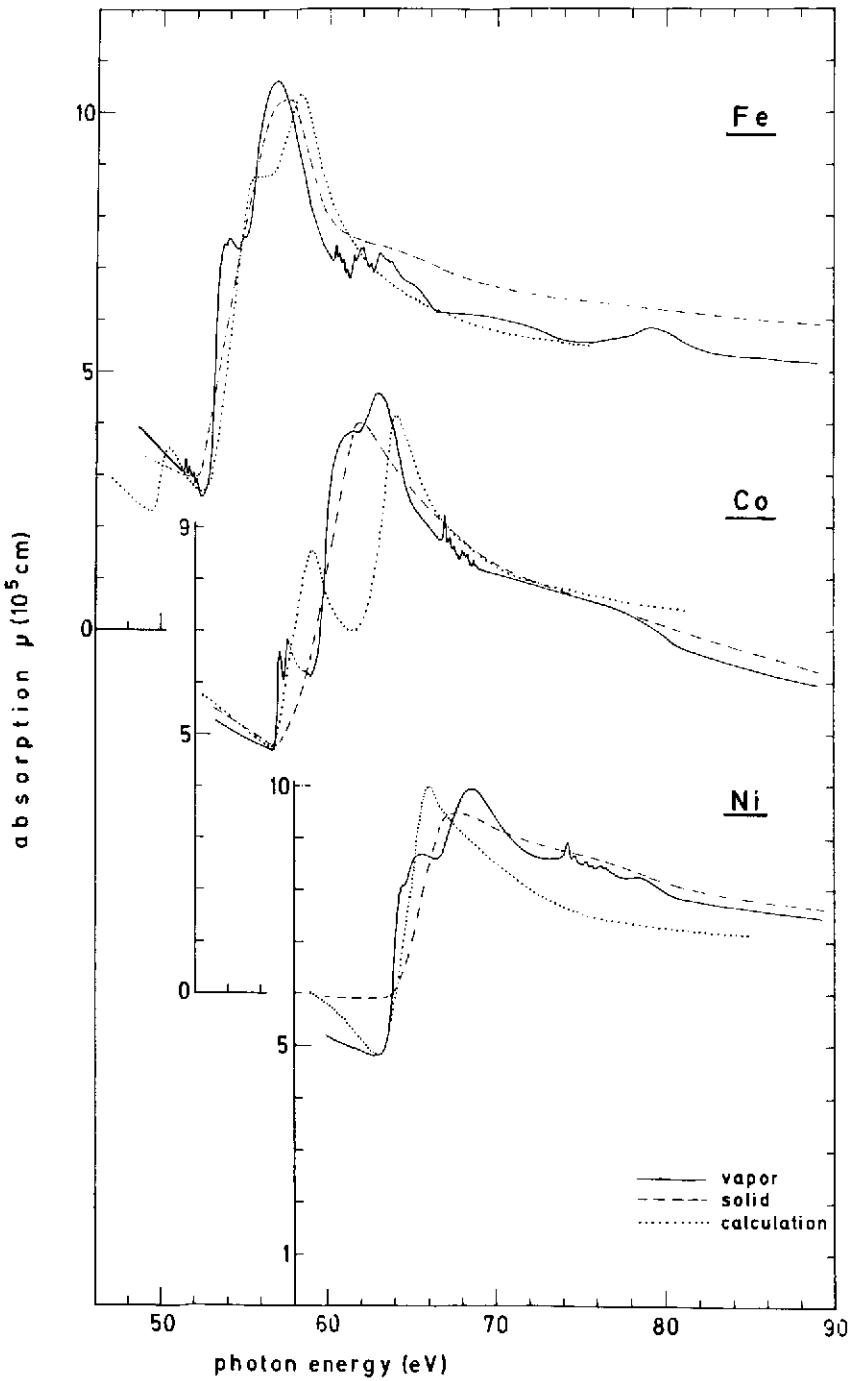
Fe
Co
Ni
absorption μ (10⁵cm)
photon energy (eV)
vapor
solid
calculation

Fig. 10